A Compromise of Comfort and Handling in Automotive Vertical Dynamics

Chatchai Chumjun[1*], Chak Chantalakhana[2] and Saiprasit Koetniyom[3]

[1] Automotive Engineering, The Sirindhon Thai-German Graduate School (TGGS)
King Mongkut's Institute of Technology North Bangkok
1518 Pibulsongkram Road Bangsue Bangkok 10800, Thailand.
*Email: tum_amt2002@hotmail.com[1]
[2, 3]Mechanical Engineering Department, Engineer Faculty,
King Mongkut's Institute of Technology North Bangkok
1518 Pibulsongkram Road Bangsue Bangkok 10800, Thailand. Tel. 02-913-2500 ext 8324
Email:chakjoe@hotmail.com[2] and saps@kmitnb.ac.th[3]

Abstract

The advantage of the anti-roll bars is to reduce the body roll acceleration and roll angle during single wheel lifting and cornering, the driving safety and handling have been affects by these parts. However, the anti-roll bar also has disadvantages. The more the spring rate related to the wheels increases and the more highly the elastic parts are pre-tensioned in the various mountings, the less the total springing responds when the vehicle is moving over a bump road. The ride comfort also deteriorates. Therefore prefect design of a passive suspension can to some extent optimize ride comfort and handling stability, but cannot eliminate this compromise.

Keyword: Vertical Dynamics, Suspension Model, Full Vehicle Model

1. Introduction

The main purpose of study is to design the suspension system of concept city car in order to achieve the optimum performance due to conflict between comfortable ride and good handling.

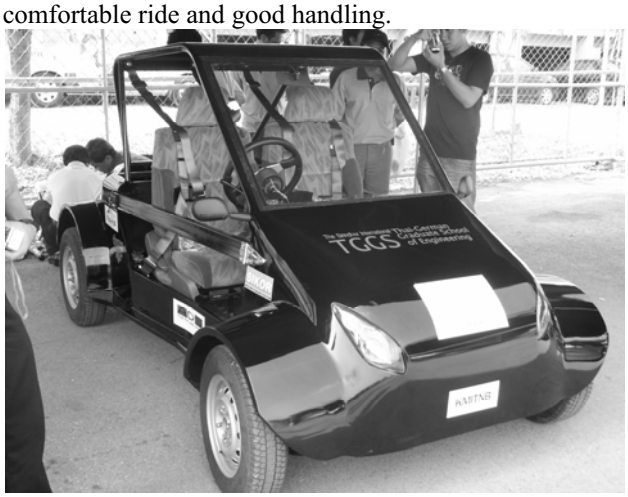

Figure 1 Concept city car in Autochallenge 2006 contest made by TGGS team.

In some situation, these characteristics can not achieve in the same time. So the complex mathematical models of suspension system are needed to explain these characteristics and study the effects of each suspension component, especially the anti- roll bar for this study. The mathematical model used in this study was a full vehicle model. This model was programming with MatLab/Simulink to study the vehicle behaviors in vertical dynamics which is adjusted the parameters very easily. The models were studied by varying the parameters and comparing the results.

.

2. Theory

2.1 Vertical dynamic study

The passive suspension system consists of mass, spring and damper, which are constant values. They have influences to ride comfort and handling of vehicle due to body acceleration, body pitch and roll acceleration. Thereby, the mathematical model of full vehicle model are used for analyzing and finding the influences from those parameters such as weight distributed, stiffness spring, damping factor and sprung mass. The natural frequencies are affected by those parameters too. These natural frequencies are very important to vehicle design, which affect to fatigue of passengers. Generally, one of the most important parts of the human body with respect to vibration and shock seems to be the abdominal part with the resonance occurring in the 4-8 Hz range [1, 2 and 3]. MacMillan [1] proposed that other main resonant effect is found in the range 20-30 Hz related to the head-neck part. Also, a vibration in the region 20-90 Hz correlates with the eyeball resonance. Above 100 Hz is not very useful, and other more complex analyses have to be used.

2.2 Full Vehicle Model 7 DOF

A mathematical model of vehicle is derived as the 7 degrees of freedom system which is enough for studying

stability performance and ride comfort as show in Figure 2.

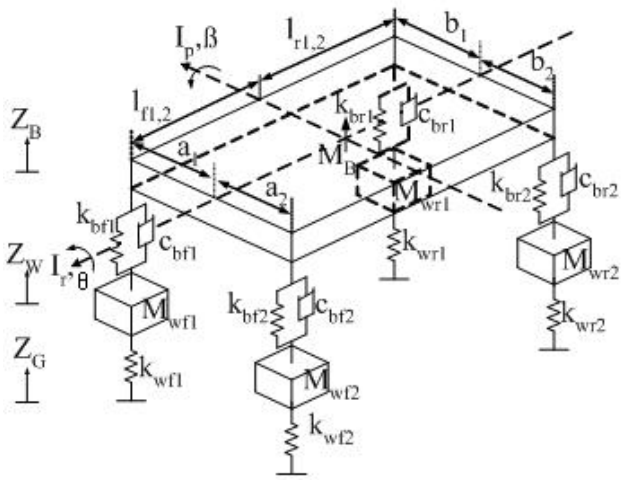

Figure 2 Full Vehicle Model

Equations of Motion for MDOF are formulated as:

Body mass

$$M_b\ddot{Z}_b+(c_{bf1}+c_{bf2}+c_{br1}+c_{br2})\dot{Z}_B-(c_{bf1}l_{f1}+c_{bf2}l_{f2}-c_{br1}l_{r1}-c_{br2}l_{r2})\dot{\beta}$$
$$-(c_{bf1}a_1-c_{bf2}a_2+c_{br1}b_1-c_{br2}b_2)\dot{\theta}-c_{bf1}\dot{Z}_{wf1}-c_{bf2}\dot{Z}_{wf2}-c_{br1}\dot{Z}_{wr1}-c_{br2}\dot{Z}_{wr2} \quad (1)$$
$$+(k_{bf1}+k_{bf2}+k_{br1}+k_{br2})Z_b-(k_{bf1}l_{f1}+k_{bf2}l_{f2}-k_{br1}l_{r1}-k_{br2}l_{r2})\beta$$
$$-(k_{bf1}a_1-k_{bf2}a_{r2}-k_{br1}b_1+k_{br2}b_2)\theta-k_{bf1}Z_{wf1}-k_{bf2}Z_{wf2}-k_{br1}Z_{wr1}-k_{br2}Z_{wr2}=0$$

Pitch

$$I_p\ddot{\beta}_b-(c_{bf1}l_{f1}+c_{bf2}l_{f2}-c_{br1}l_{r1}-c_{br2}l_{r2})\dot{Z}_B+(c_{bf1}l_{f1}^2+c_{bf2}l_{f2}^2$$
$$+c_{br1}l_{r1}^2+c_{br2}l_{r2}^2)\dot{\beta}+(c_{bf1}l_{f1}a_1-c_{bf2}l_{f2}a_2-c_{br1}l_{r1}b_1+c_{br2}l_{r2}b_2)\dot{\theta}$$
$$+c_{bf1}l_{f1}\dot{Z}_{wf1}+c_{bf2}l_{f2}\dot{Z}_{wf2}-c_{br1}l_{r1}\dot{Z}_{wr1}-c_{br2}l_{r2}\dot{Z}_{wr2}-(k_{bf1}l_{f1}+k_{bf2}l_{f2} \quad (2)$$
$$-k_{br1}l_{r1}-k_{br2}l_{r2})Z_B+(k_{bf1}l_{f1}^2+k_{bf2}l_{f2}^2+k_{br1}l_{r1}^2+k_{br2}l_{r2}^2)\beta$$
$$-(k_{bf1}l_{f1}a_1-k_{bf2}l_{f2}a_2-k_{br1}l_{r1}b_1+k_{br2}l_{r2}b_2)\theta-k_{bf1}Z_{wf1}-k_{bf2}Z_{wf2}$$
$$-k_{br1}Z_{wr1}-k_{br2}Z_{wr2}=0$$

Roll

$$I_r\ddot{\theta}_b-(c_{bf1}a_1-c_{bf2}a_2+c_{br1}b_1-c_{br2}b_2)\dot{Z}_B+(c_{bf1}a_1l_{f1}-c_{bf2}a_2l_{f2}$$
$$-c_{br1}b_1l_{r1}+c_{br2}b_2l_{r2})\dot{\beta}+(c_{bf1}a_1^2+c_{bf2}a_2^2+c_{br1}b_{r1}^2+c_{br2}b_2^2)\dot{\theta}$$
$$+c_{bf1}a_1\dot{Z}_{wf1}-c_{bf2}a_2\dot{Z}_{wf2}-c_{br1}b_1\dot{Z}_{wr1}+c_{br2}b_2\dot{Z}_{wr2}-(k_{bf1}a_1-k_{bf2}a_2 \quad (3)$$
$$-k_{br1}b_1+k_{br2}b_2)Z_B+(k_{bf1}a_1l_{f1}-k_{bf2}a_2l_{f2}-k_{br1}b_1l_{r1}+k_{br2}b_2l_{r2})\beta$$
$$+(k_{bf1}a_1^2+k_{bf2}a_2^2+k_{br1}b_1^2+k_{br2}b_2^2)\theta+k_{bf1}a_1Z_{wf1}-k_{bf2}a_2Z_{wf2}$$
$$-k_{br1}b_1Z_{wr1}+k_{br2}b_2Z_{wr2}=0$$

Wheels

$$M_{wf1}\ddot{Z}_{wf1}-c_{bf1}\dot{Z}_B+c_{bf1}l_{f1}\dot{\beta}+c_{bf1}a_1\dot{\theta}+c_{bf1}\dot{Z}_{wf1}-k_{bf1}Z_b \quad (4)$$
$$+k_{bf1}l_{f1}\beta+k_{bf1}a_1\theta+(k_{bf1}+k_{wf1})Z_{wf1}=k_{wf1}Z_{Gf1}$$

$$M_{wf2}\ddot{Z}_{wf2}-c_{bf2}\dot{Z}_B+c_{bf2}l_{f2}\dot{\beta}-c_{bf2}a_2\dot{\theta}+c_{bf2}\dot{Z}_{wf2}-k_{bf2}Z_b \quad (5)$$
$$+k_{bf2}l_{f2}\beta-k_{bf2}a_2\theta+(k_{bf2}+k_{wf2})Z_{wf2}=k_{wf2}Z_{Gf2}$$

$$M_{wr1}\ddot{Z}_{wr1}-c_{br1}\dot{Z}_B-c_{br1}l_{r1}\dot{\beta}-c_{br1}b_{r1}\dot{\theta}+c_{br1}\dot{Z}_{wr1}-k_{br1}Z_b \quad (6)$$
$$-k_{br1}l_{r1}\beta-k_{br1}b_{r1}\theta+(k_{br1}+k_{wr1})Z_{wr1}=k_{wr1}Z_{Gr1}$$

$$M_{wr2}\ddot{Z}_{wr2}-c_{br2}\dot{Z}_B-c_{br2}l_{r2}\dot{\beta}+c_{br2}b_2\dot{\theta}+c_{br2}\dot{Z}_{wr2}-k_{br2}Z_b \quad (7)$$
$$-k_{br2}l_{r2}\beta+k_{br2}b_2\theta+(k_{br2}+k_{wr2})Z_{wr2}=k_{wr2}Z_{Gr2}$$

2.3 Road surface

The shape of the obstacle, used as displacement excitation to the vehicle model, is approximated by a smooth function, like a cosine half wave [5], then, discontinuities will be avoided. Usually the obstacles are described in local reference frames, as shown in Figure 3.

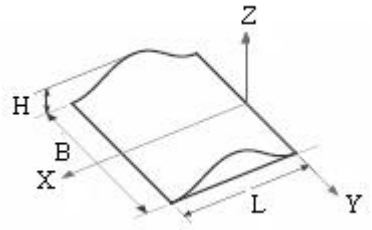

Figure 3 cosine-shaped bump[5].

The cosine-shaped bump is given

$$z(x,y)=\begin{cases}\frac{1}{2}H\left(\cos\left(2\pi\frac{x}{L}-\phi\right)+1\right) & if\ 0<x<L\ and \\ & -\frac{1}{2}B<y<\frac{1}{2}B \\ 0 & else\end{cases} \quad (8)$$

H (m), B (m) and L (m) denote height, width and length of the obstacle, respectively. The angle $\emptyset$ is to describe a phase lag.

2.4 Anti Roll bar Model

From the full vehicle model, an anti-roll bar is connected the vertical movements on both the front and rear wheels. Torsional rotation is generated at both ends of the bar by vertical movement of sprung mass. The equation of motion of the system is modified when the anti-roll bar is considered and, moreover, additional equation corresponding to the torsional DOF of the anti roll bar is formulated [6]. The rotational inertia of the anti-roll bar is not considered here.

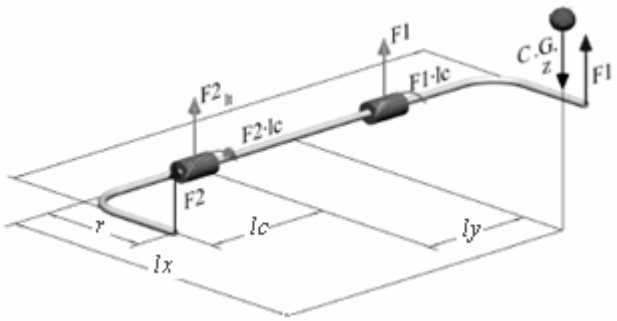

Figure 4. Anti-roll bar with the applied force at the sprung and unsprung masses and their translation at the fixing points of the bar and the C.G. of vehicle[6].

Anti-roll bar action caused by single wheel lift

$$\frac{d\alpha_f}{dt}=\frac{1}{r_f}(z_{wf2}-2(l_{cf}+l_{yf})\theta-z_{wf1}) \quad (9)$$

$$\frac{d\alpha_r}{dt}=\frac{1}{r_r}(z_{wr2}-2(l_{cr}+l_{yr})\theta-z_{wr1}) \quad (10)$$

α_f, α_r, = Angle of tip anti roll bar both front and rear suspension

Front right wheel mass in vertical movement

$$M_{wf1}\ddot{Z}_{wf1} = original\ \ equation + \frac{k_{sf}\alpha_f}{r_f} \quad (11)$$

Front left wheel mass in vertical movement

$$M_{wf2}\ddot{Z}_{wf2} = original\ \ equation - \frac{k_{sf}\alpha_f}{r_f} \quad (12)$$

Rear right wheel mass in vertical movement

$$M_{wr1}\ddot{Z}_{wr1} = original\ \ equation + \frac{k_{sr}\alpha_r}{r_r} \quad (13)$$

Rear left unsprung mass in vertical movement

$$M_{wr2}\ddot{Z}_{wr2} = original\ \ equation - \frac{k_{sr}1\alpha_r}{r_r} \quad (14)$$

Body mass in roll movement

$$I\ddot{\theta} = original\,equation + \frac{2(l_{yf}+l_{cf})k_{sf}\alpha_f}{r_f} + \frac{2(l_{yr}+l_{cr})k_{sr}\alpha_r}{r_r} \quad (15)$$

Body mass in vertical movement

$$M_b\ddot{Z}_b = original\ \ equation + \frac{2l_{yf}k_{sf}\alpha_f}{r_f} + \frac{2l_{yr}k_{sr}\alpha_r}{r_r} \quad (16)$$

Anti-roll bar action caused by the body roll

$$\theta = \frac{2.\Delta h}{K_{bf}.S_{sf}{}^2 + K_{stab}.S_{stab\,f}{}^2 . + K_{br}.S_{sr}{}^2 + K_{stab}.S_{stab\,r}{}^2}.F_{Lat,b} \quad (17)$$

Where:

$S_{sf,r}$ = Spring track width in front, rear (N/m)
$K_{bf,r}$ = Body spring stiffness in front, rear (N/m)
Δh = Distance between CG and roll center (m)
$F_{lat,b}$ = Lateral Force (N)
v = Velocity (m/s)
R = radius of curve (m)
$K_{stabf,r}$ = Anti roll bar stiffness in front, rear (Nm/rad)
$S_{stabf,r}$ = Anti roll bar track width in front, rear (m)

2.5 Simulation conditions

The conditions for simulation are summarized in Table 1. These vehicle specification data is provided by students of The Sirindhon Thai-German Graduate School (TGGS), KMITNB from competition in Autochallenge 2006 contest, organized by Society of Automotive Engineers - Thailand (TSAE).

Table 1 Specification data by concept city car

Symbol	Description	Value
M_b	Sprung mass	290 kg
m_{wf1}, m_{wf2} m_{wr1}, m_{wr2}	Unsprung mass of each wheel	15 kg
l_{f1}, l_{f2} l_{r1}, l_{r2}	Length of C.G between front and rear of vehicle	0.9 m 1.1 m
I_p I_r	Pitch and Roll axis moment of inertia	287.1 Kg-m^2 128.631 Kg-m^2
a_1, a_2 b_1, b_2	width of left and right sprung mass	0.665m 0.667m
k_{bf1}, k_{bf2} k_{br1}, k_{br2}	Spring stiffness of front and rear suspension	8760.33 N/m 9810 N/m
c_{bf1}, c_{bf2} c_{br1}, c_{br2}	Damping ratio of front and rear suspension	ζ = 0.3 956.3360 Ns/m
k_{wf1}, k_{wf2} k_{wr1}, k_{wr2}	Tire stiffness	130000 N/m
k_{sf} k_{sr}	Anti roll bar stiffness front and rear wheel	28449 Nm/rad 28449 Nm/rad
r l_{yf} l_{cf} l_{xf} l_{yr} l_{cr} l_{xr}	Anti roll bar dimensions, see Figure 4.	0.22 m 0.27 m 0.3 m 1.1 m 0.27 m 0.3m 1.32 m
h r_r R	CG height Roll center Wheel radius	0.45 m 0.19 m 0.2684 m
Z_B	DOF of sprung mass	
β	DOF of pitch	
Θ	DOF of roll	
Z_{wf1}	DOF of Front right wheel mass	
Z_{wf2}	DOF of Front left wheel mass	
Z_{wr1}	DOF of rear right wheel mass	
Z_{wr2}	DOF of rear left wheel mass	
Z_G	Road surface	

The condition determines vehicle behavior under constant car speed, ds/dt = v, the momentary position of the vehicle is given by s = v_t, where the initial position s = 0 at t_S = 0 are determined. The t_L denotes the time delay of bump and t_S the time delay between front and rear wheel give by L/v. The angle $\varnothing$ is to describe a phase lag between the front and the rear wheel, then phases of front and rear wheels are π and $\pi - 2\pi t_S/t_L$, respectively. Obstacle dimension is that B = 0.5, H =0.1 m and L=1 m.

For body roll simulation, running on a circular track of fixed radius of 25, 50 and 100 m at different velocities are used. The entrance velocity is controlled to obtain the centrifugal force desired.

3 Simulation study

If one of a pair of wheels lifts as passing over a bump in the road (cosine shaped bump), then the vertical deflection of the wheel and spring raises and rotates the anti-roll bars cranked arm on that side so that the transverse span of the bar is twisted. These provide a torque which is proportional to angle of rotation. This torque is transferred to the opposite cranked arm which then applies a downward force onto the wheel. However, because the wheel cannot sink into the ground, the reaction occurs on mounting point which therefore tends to lift up the side of the body on the opposite side to the vertically deflected wheel. As a result, both sides of the body mass will have been raised, thereby enabling the vehicle body to remain upright instead of tilting to one side. In the simulation results, it showed the body

responses in time domain of vehicle at speeds 22.5 to 90 km/hr.

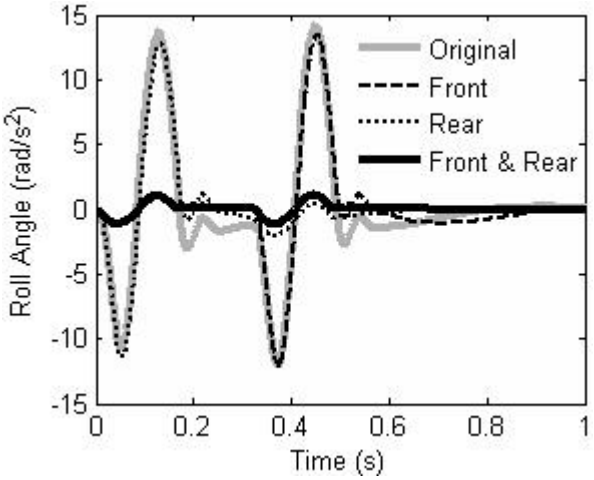

Figure 5 Roll angle of sprung mass at 22.5 km/hr.

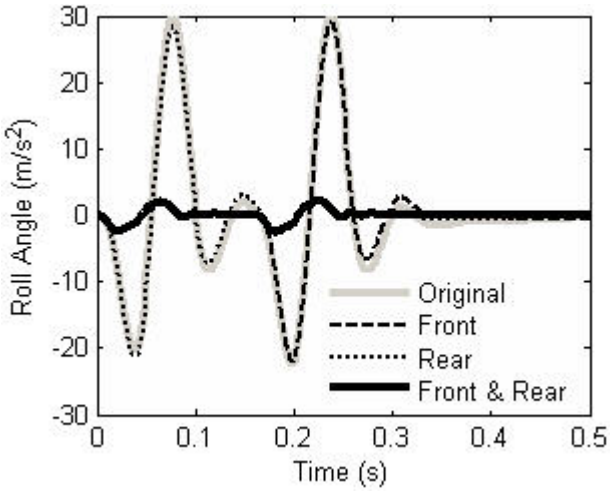

Figure 6 Roll angle of sprung mass at 45 km/hr.

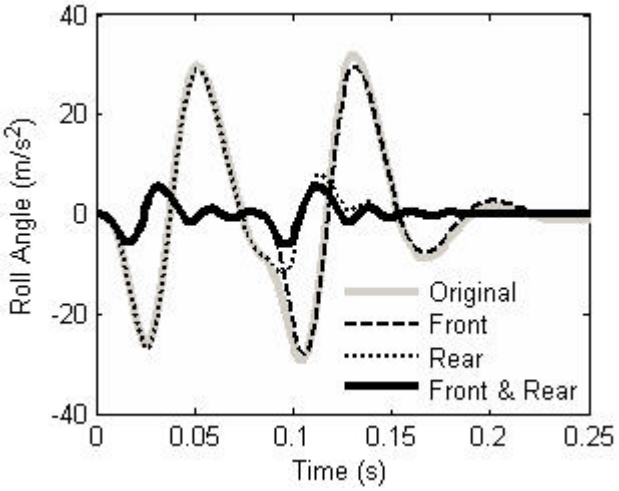

Figure 7 Roll angle of sprung mass at 90 km/hr

In Figures 5, 6 and 7, the roll acceleration of vehicle body has being more reduced by anti roll bar which install in front and rear wheel and fast approach to steady state. The installation only one part in front or rear wheel affected nearly of amplitude peaks and same time to steady state with original case. In front only install case first amplitude is equal to front and rear installs but second amplitude is same as original case. In the opposite rear only install first amplitude is equal to original case and but second amplitude is same as front and rear install.

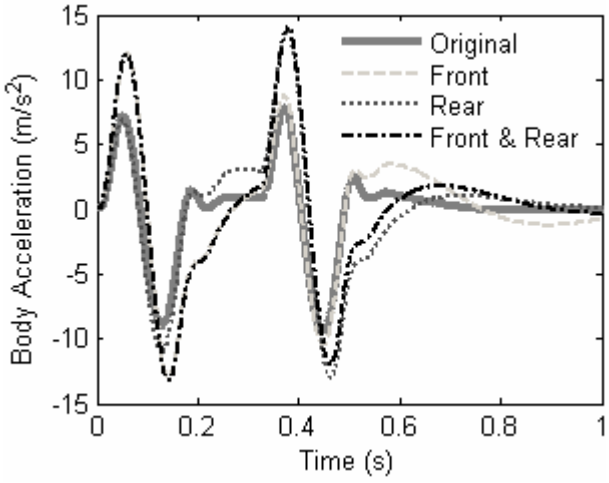

Figure 8 Body movements at 22.5 km/hr

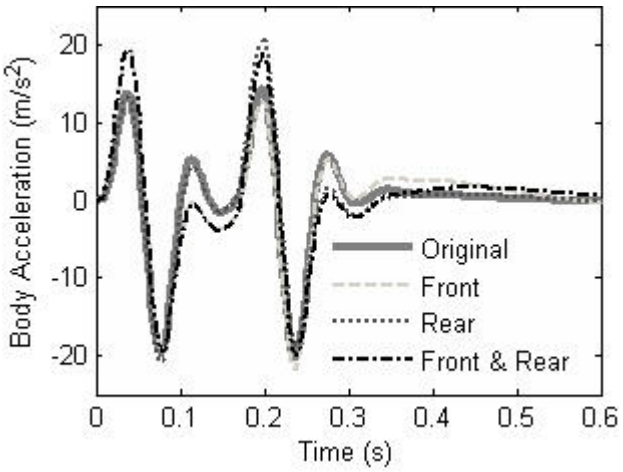

Figure 9 Body movements at 45 km/hr

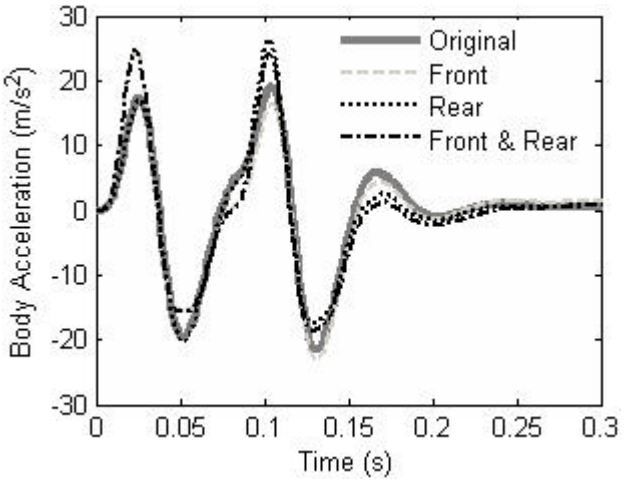

Figure 10 Body movements of sprung mass at 90 km/hr

The acceleration in z-direction of car body has a same trend for low and high speed; only the amplitudes are difference (see Figures 8, 9 and 10), therefore, properties of passive suspension has mechanical filter, which is good response for low speed,. In this part, anti-roll bar is installed in both front and rear caused more spring rate and more lift up than only front or rear installed, while pass over bump profile at 22.5 km/hr the anti-roll bar make sluggish approach to steady state and more acceleration amplitude because of more spring rate, which is affect to uncomfortable. As the vehicle pass over bump profile at 45 and 90 km/hr, this part have same approach to steady stat. In case acceleration amplitude of anti-roll bar makes more value than original type.

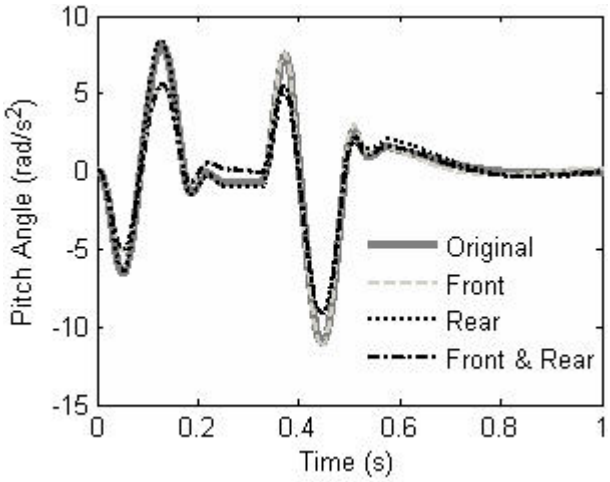

Figure 11 Pitch angle of body mass at 22.5 km/hr

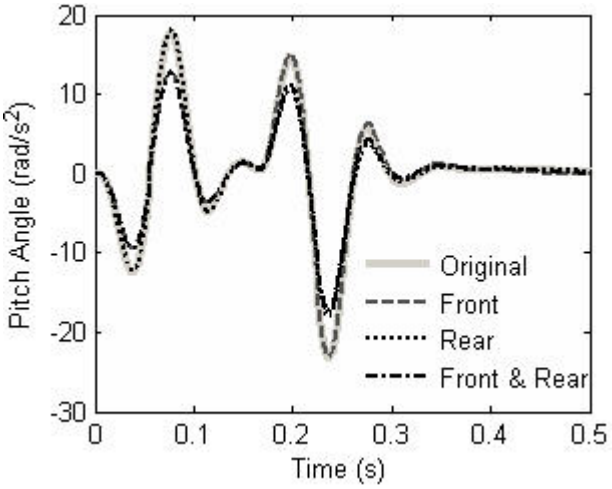

Figure 12 Pitch angle of body mass at 45 km/hr

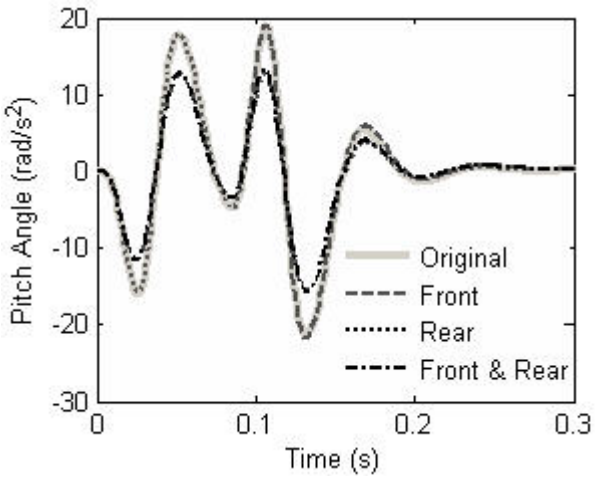

Figure 13 Pitch angle of body mass at 90 km/hr

The results showed that the anti-roll bar applied at both front and rear wheels have lower pitch acceleration amplitude than other cases but same time approach to steady stat (e.g. only rear installed, and not-install). (See figures 11, 12 and 13). In front only install case first amplitude is equal to front and rear installs but second amplitude is same as original case. On the other hand, rear only install, first amplitude is equal to original case and second amplitude is same as front and rear install.

Summarizing the of time response of influent of anti roll bars. The anti-roll bar is incorporated into the suspension of a vehicle to enable low rate soft springs to be used which provides a more comfortable ride under normal driving conditions. This bar does not contribute to the suspension spring stiffness, the suspension's resistance to vertical deflection, as its unsprung weight is increased or when the driven vehicle is subjected to dynamic shock loads caused possibly by gaps or ridges where concrete sections of the road are joined together. However, the anti-roll bar does become effective if one wheel is raised higher than the other as the vehicle passes over a bump in the road. Under these conditions, the suspension spring stiffness (total spring rate) increases in direct proportion to the relative difference in deflection of each pair of wheels when subjected to the bump and rebound of individual wheels.

ISO 2631 exposure limit for whole body vibration exposure for 1 min duration is 8 m/s^2 (rms) acceleration at the about 2 Hz range and the BS 6841 standard for 1 s duration is 28 m/s^2 [7]. The trend shows that the limits are likely to be higher for shorter durations.

Figure 14 shows the frequency spectrum for the vertical acceleration of centre of gravity of vehicle while passing over bump with 22.5 km/hr. Dominant frequency of 2-4 Hz has amplitude of acceleration equal to 0.085 m/s^2, 0.1442 m/s^2, 0.102 m/s^2 and 0.1735 m/s^2.

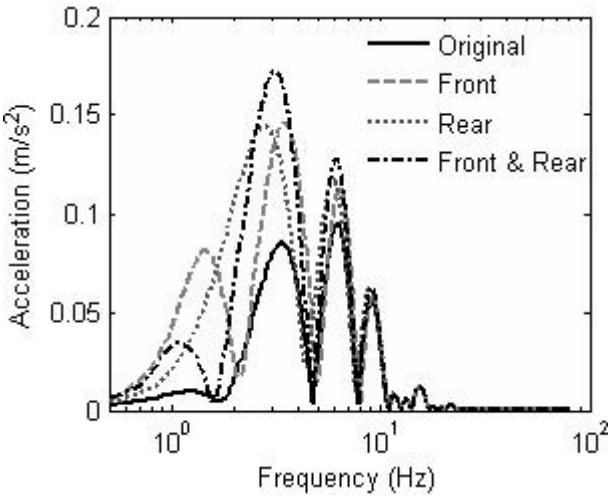

Figure 14 Frequency spectrum of vertical acceleration at 22.5 km/hr .

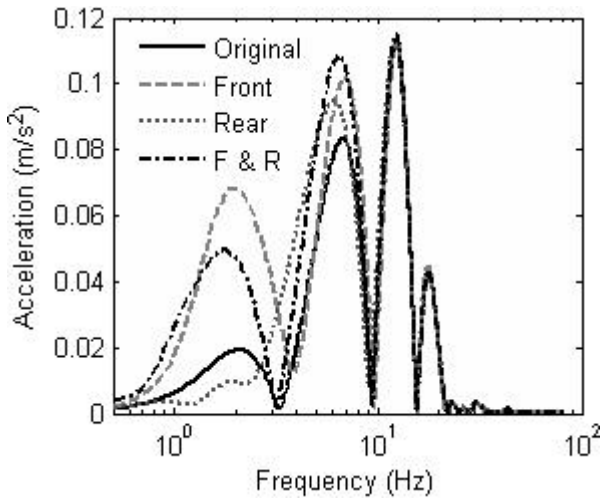

Figure 15 Frequency spectrum of vertical acceleration at 45 km/hr.

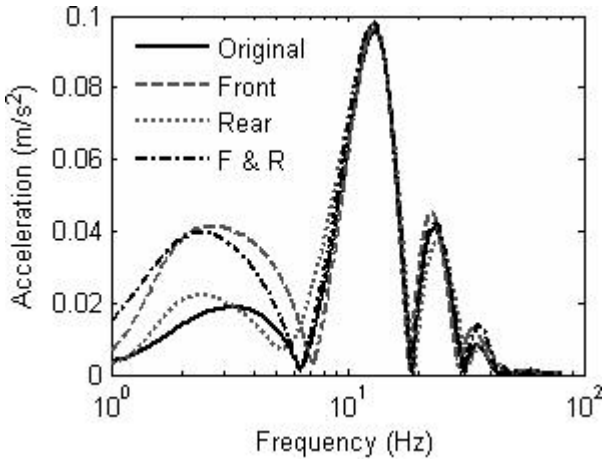

Figure 16 Frequency spectrum of vertical acceleration at 90 km/hr.

Figure 15 shows the frequency spectrum for the vertical acceleration of centre of gravity of vehicle while passing over bump with 45 km/hr. Dominant frequency of about 2 Hz range has amplitude of acceleration equal to 0.019 m/s^2, 0.0682 m/s^2, 0.0095 m/s^2 and 0.0495 m/s^2 respectively.

Figure 16 shows the frequency spectrum for the vertical acceleration of centre of gravity of vehicle while passing over bump with 90 km/hr. Dominant frequency of 2-4 Hz have amplitude of acceleration equal to 0.02 m/s^2, 0.022 m/s^2, 0.04 m/s^2 and 0.042 m/s^2 respectively.

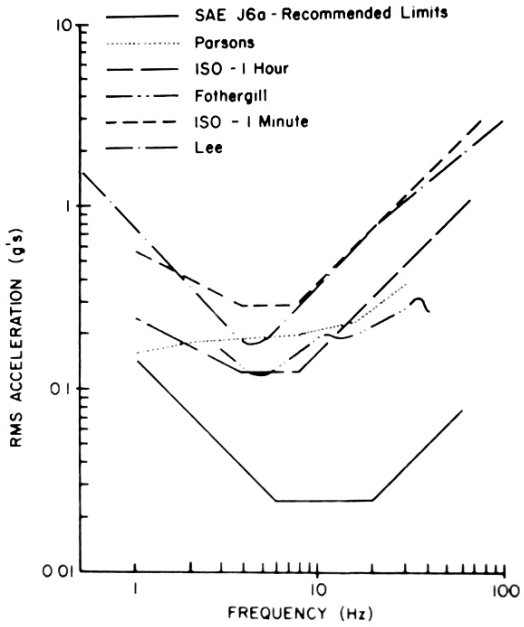

Figure 17 Human tolerance limits for vertical vibration [4]

Figure 17 shows lines of constant comfort as determined by many researchers [4]. Because of the different interpretation of comfort in each study the nominal level of one curve is not comparable to the others, nor is it especially meaningful.

Summarizing the results of frequency spectrum analysis, the dominant frequency is approximately 2 Hz with amplitude of acceleration varying at 22.5 km/hr between 0.085 m/s^2 to 0.1735 m/s^2, at 45 km/hr between 0.019 m/s^2 to 0.0495 m/s^2 and at 90 km/hr between 0.02 m/s^2 to 0.042 m/s^2 for the cosine shaped bump profiles considered. Further, the vehicle passing over the bumps simulated is not likely to exceed tolerance limits as stated for whole body vibration. In case of optimization only for comfort, it's not need to use the anti-roll bar which has to trade off with more acceleration.

Figures 18, 19 and 20 shows roll angle of the three models. For speed lower than the differences are not important and for velocity of 25 m /s (90 km/hr) the tendency of differences angle is about 66 percents between without anti-roll bar and with single front or rear anti-roll bar as well as the differences angle is 80 percents between without anti-roll bar and with dual front and rear anti-roll bar. One of the functions that are commended to

the anti-roll bar is the decrease of the body roll angle under lateral force.

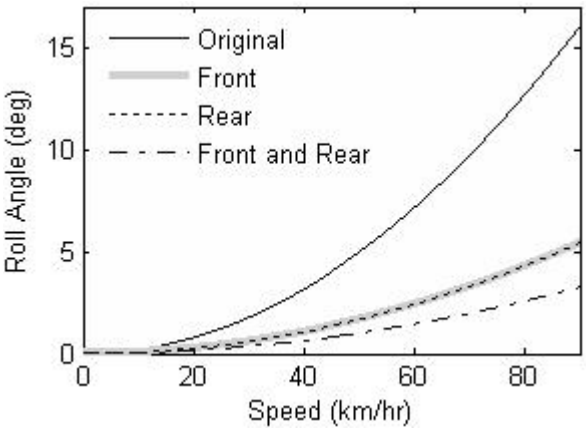

Figure 18 Roll angle (degree) and curve circulation speed with assumption: v = 0-25 m/s (0-90 km/hr), r =25 m

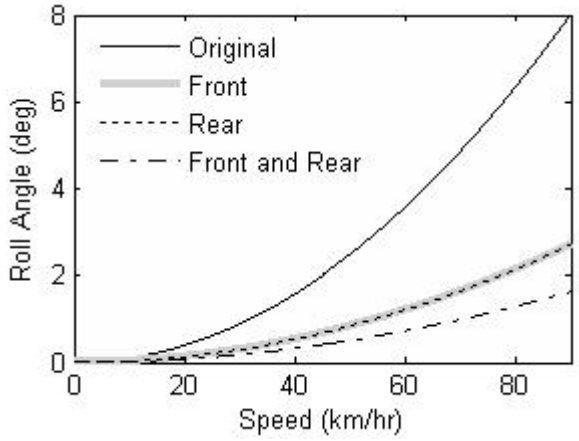

Figure 19 Roll angle (degree) and curve circulation speed with assumption: v = 0-25 m/s (0-90 km/hr), r =50 m

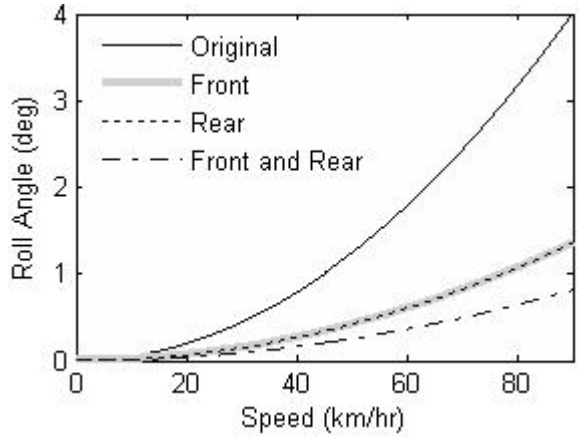

Figure 20 Roll angle (degree) and curve circulation speed with assumption: v = 0-25 m/s (0-90 km/hr), r = 100 m

4. Conclusion

The anti-roll bar can decrease the body roll angle under lateral force during the cornering and single wheel lifting at difference speed. As can be seen from the results, the vehicle with the anti roll bar develops much lower angle of body roll. Therefore the benefits of anti roll bar to provide additional handling stability and a more level ride comfort. In case of experimental test and ride and handling evaluate will be further investigated.

Acknowledgment

The first author is being supported by College of Industrial Technology (CIT), KMITNB.

The vehicle specification data is provided by The Sirindhon Thai-German Graduate School (TGGS), KMITNB.

5. Reference

[1] Renata MacMillan.,"Basic Characteristics of Human Vibration" Warsaw Technical University. http://www.safetyline.wa.gov.au/institute/level2/course19/lecture59/l59_01.

[2] D.A. Crolla, G.Firth, D. Horton., "An Introduction to Vehicle Dynamics" Department of Mechanical Engineering, University of Leeds, UK.

[3] Henning Wallentowitz., 2003. "Vertical and Lateral Dynamics" Kraftfahrwesen Aachen of RWTH Aachen University, Germany,

[4] Thomas D. Gillespie.,1992 "Fundamentals of Vehicle Dynamics", Society of Automotive Engineers, Inc.

[5] Georg Rill.,2005 "Vehicle Dynamics" Fachhochschule Regensburg University of Applied Sciences Hochschule für Technik Wirtschaft Soziales, Germany.

[6] Mera.J.M, Vera, J. Fe'lez, J.J.Esperilla, "Influence of the Roll Axis Consuderation in Vehicle Dynamics. Bond Graph Models" GIGS E.T.S.I Industiales, Universidad Polite′cnica de Madrid Spain

[7] T R Gawade, Dr S Mukherjee and Prof D Mohan.,2004 "Wheel Lift-off and Ride Comfort of Three-wheeled Vehicle over Bump"Department of Mechanical Engineering, IIT Delhi, New Delhi India.